

Simulation and Implementation of a Poly Methyl Methacrylate based Whispering Gallery Mode Ring Resonator in Microwave Range

A. Malekpour, A. Rostami, M. Sarmadi, M. Dolatyari and G. Rostami

OIC Research Group, School of Engineering-Emerging Technologies, University of Tabriz, Tabriz 5166614761, Iran

Keywords: Ring Resonator, Poly Methyl Methacrylate (PMMA), Whispering Gallery Mode, Microwave Frequency.

Abstract: This article introduces the ring resonator sensing principle and presents the simulation and fabrication of a ring resonator structure. The material Poly methyl methacrylate (PMMA) with refractive index of 1.5 has been used for fabricating it. It has low loss and thereby is a good material for constructing low loss ring resonators and generating high Q-factors. 3-D finite element numerical method (FEM) simulation results show the path of light through ring resonator and the transmission parameter of a waveguide in close proximity of a ring resonator. After coupling electromagnetic wave from the waveguide into the ring resonator, the standing waves are formed as resonant optical modes. Subsequently resonance peaks are formed in periodically repetitive frequencies in the transmission parameter of the waveguide. Transmission spectrum of waveguide has been studied in the frequency range 8-8.3 GHz. Ring resonator parameters like free spectral range and quality factor have been calculated by 0.1245 GHz and 200 respectively. Agreement and differences between simulation and experiment have been discussed.

1 INTRODUCTION

Whispering gallery modes (WGMs) are specific resonances of a wave field, inside a given resonator or a cavity with smooth edges. The resonators have axially symmetric geometry such as sphere, disk or ring. WGMs can be described as propagating modes circling around the resonator, supported by continuous total internal reflection of the resonator or cavity surface, that meet the resonance condition. This means that after one round trip they return to the same point with the same phase shift of integer multiples of 2π . Hence the waves interfere constructively with themselves, and form standing waves.

The operating principle in ring resonator based sensors is mainly based on resonance perturbation method, where a sample under test perturbed the effective refractive index of the resonator (Zhu, Hongying, 2007, Delâg, 2009). Resonance field perturbs by the refractive index changes and causes a change in the resonance frequency and Q-factor. Other perturbation in resonance frequency is caused by the attachment of a desirable particle (Ahmadi, 2014). These changes can be calibrated to represent the sensing parameters of interest. This is an example

of RI sensors that involves detecting the spectral shift of a resonance feature as the RI varied. The other approaches of such RI sensors are valid and have a wide range of applications in areas such as life science (Yu. Zongfu, 2011). Yet the most interesting from a practical viewpoint about electromagnetic WGMs, is that they possess many unique properties, such as ultra-high Q-factors, having low mode volumes and operating at optical and telecommunication frequencies of light. So WGM is one of the most accurate and sensitive techniques proposed to date for sensing applications due to its sensitivity and selectivity.

High unloaded Q-factor is mainly limited by the loss tangent of the resonator material for highly confined modes. Hence choosing very low loss materials such as poly methyl methacrylate (PMMA) is of paramount importance. Depending on where the sensing signal originates, there are two types of sensing that a ring resonator can accomplish. The sample under test in close proximity to the ring resonator surface (much closer than the evanescent field decays length) performs the surface sensing signal. Whereas bulk sensing signals come from the optical change induced by the presence of the sample in the whole region of the evanescent field. Placing and removing the sample at predetermined location

close to the resonator, is very easy due to open structure of a WGM structure, unlike metallic cavity. In addition, at microwave range of the electromagnetic spectrum, whispering gallery resonators have relatively large dimensions and therefore, they are easy to handle and manipulate. By this idea, the structure becomes suitable for mass production, because the time consuming part of manual adjustment is eliminated.

In this paper we have presented the simulation results and the fabricated ring resonator structure using PMMA that creates peak resonances in microwave range. PMMA is considered one of the best materials to exhibit the lowest loss. Hence high unloaded Q-factor can be achieved. The gap between waveguide and resonator is an important factor for the ring resonator. Since the field distribution is weak in the middle hole at microwave range, it is not sensitive sensor if the sample filled the core of the ring resonator. Placing the sample in the vicinity of the outer rim of the resonator is not possible, because there is no limitation for the liquid to remain in the vicinity. For having got a good performance sensor, it's a good idea to implement a groove at the ring's surface and near the outer rim of the resonator. This idea is practical and in the future we will have done it.

2 THEORY AND FORMULATION

It is known from the waveguide-based optics that occurring total internal reflection on the border of core and clad is the basically condition for generating waveguide structures (Taya. Sofyan, 2014). The reflected waves interfere constructively with each other and the modes are formed and propagated in the waveguide. So the larger RI of the core than the RI of the clad is an essential condition for confinement of the wave in the core and formation of the propagating modes in waveguides.

Waveguide cut-off frequency depends on the effective RI and the dimensions of the waveguide. Unlike the slab waveguides, in the rectangular waveguides, there is no precise formula for wave propagation in the waveguide. After a simple and meaningful approximation, has been performed on the solving Maxwell's equations in rectangular waveguides, formulas have been obtained and tables have been presented for a rectangular waveguide (Marcatili, Enrique, 1969). So the correct dimensions for a waveguide with predetermined RI are obtained. It is seen that, by keeping the effective refractive index constant, as the dimensions become larger, the

cut-off frequency of the waveguide shift to lower frequencies. The dimensions of the waveguide are about the wavelength of the propagating mode in that. So for getting a waveguide at frequency 8GHz the waveguide dimensions are in the range of centimetre (cm), because wavelength at this range is about 3 cm.

This is also the case for ring resonator. If the ring resonator is considered as the curved waveguide, wave propagation in it, is the same as for the straight waveguide. The difference between them is that there are losses due to curved boundaries in ring resonator. The resonance modes are in the wavelength λ , which is given by (Sun, Yuze, 2011):

$$\lambda_r = 2\pi r n_{eff} / m \quad (1)$$

Where r is the resonator rim, n_{eff} is the effective RI experienced by the optical resonant mode, and m is an integer number. One important parameter is the distance between resonance peaks, which is called the free spectral range (FSR). The relation between the FSR and the radius of the ring resonator and effective RI is given by (Rabus. Dominik G, 2007):

$$FSR = \lambda_r^2 / 2\pi r n_{eff} \quad (2)$$

It can be seen that the FSR have a direct relationship with square of the wavenumber and an inverse relationship with the effective RI and the radius of the ring resonator. So it is expected that if the structure is at microwave range the FSR would decrease by decreasing the wavelength.

Achieving a narrowness of the resonance dip in figure 1 is an important issue in the sensor applications of ring resonator. The parameter of importance is the resonance width at half maximum or 3 dB bandwidth $\delta\lambda_r$ of the resonance lineshape.

The narrowness of linewidth $\delta\lambda_r$ is characterized by the resonator's quality factor. This parameter is a measure of the sharpness of the resonance. It is defined as the ratio of the operation wavelength and the resonance width:

$$Q = \lambda_r / \delta\lambda_r \quad (3)$$

Not too surprisingly, Q can be shown to be proportional to the number of round trips that circulating resonant light can make along the ring resonator. The quality factor can also be regarded as the stored energy divided by the power lost per optical cycle. As the detection of the ring resonator based sensors limit is set by how well one can locate resonance frequency, the sharpness is important and

a high Q is essential.

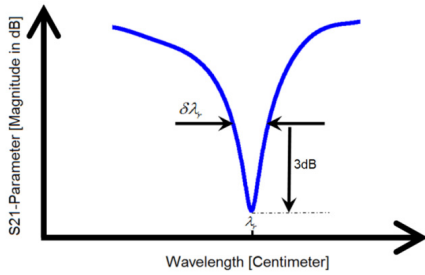


Figure 1: Exhibition of the linewidth in a resonance frequency for calculating the quality factor. .

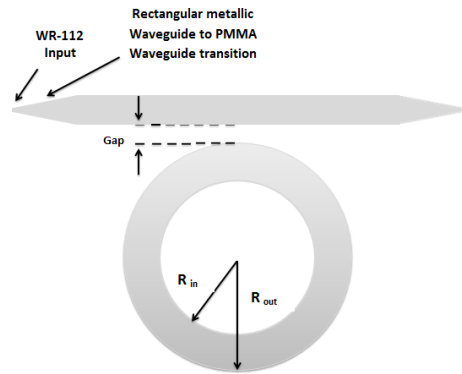


Figure 2: The top view of waveguide and ring resonator structure.

3 DESIGN AND SIMULATION OF THE STRUCTURE

The top view of the structure that consists of a PMMA waveguide and a PMMA resonator is shown in Figure 2. The ring and the waveguide have the same height 1.5 cm. The cross sectional dimensions of the waveguide are chosen to be 1.5 cm by 3.2 cm to excite the fundamental mode E_{11}^y .

The inner and outer radii of the ring are 15 cm and 24 cm respectively. The gap is chosen to be zero in simulation and also in the experimental test to have a good coupling at 8-8.3 GHz. In addition here a groove is implemented in the surface of the ring for sensing applications of the structure that we will have in the future works. It is considerable that this groove has effects on the resonance frequency. So resonance frequencies are different from the situation that there is no groove on the ring's surface. In order to keeping up the agreement between simulation and fabrication a groove has been added to the ring's surface in the simulation. Having accurate measurement and characterization, we need standard ports. So the two ends of the PMMA waveguide are tapered and inserted in WR-112, standard rectangular metallic waveguide at 7.05-10.0 GHz band.

The entire structure is simulated in CST MICROWAVE Studio 12.0, a finite element solver, to solve for the electric field distribution and the transmission parameter of the ring resonator structure. The simulated distribution of electric field in the waveguide and resonator are shown in Figure 3.

The transmission parameter of the structure which is shown in figure 4 shows that the transmission from one side to another of the waveguide is good, except for the frequencies that are the resonance frequency of ring resonator. It shows that the FSR of the ring

resonator is about 0.13 GHz and the Q-factors are about 1100 for resonance peaks and they are a bit different for each resonance peak.

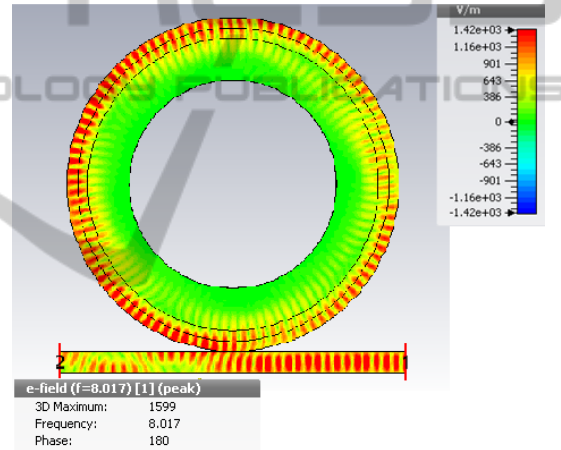


Figure 3: Distribution of absolute electric field over the PMMA ring resonator beside the PMMA waveguide at resonance frequency 8.017.

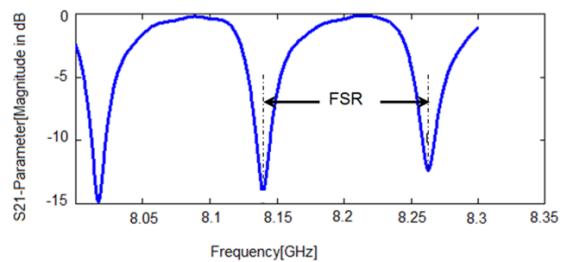


Figure 4: Transmission parameter of the PMMA structure in the simulation.

4 FABRICATION

Despite of the previous ring resonator structures

dimensions, the present case here, have centimetre dimensions. So fabricating of it, is easy, practical and affordable, and has no time consuming. There is no need for complicated technologies like the dark room or photolithography for fabrication. A PMMA slab with 1.5 cm height has been cut by laser such that a waveguide and a ring have been created. The vertical and horizontal cuttings of the two tapered ends of the waveguide are done by the former way and computer numerical control (CNC) milling machine respectively. Since both the waveguide and the ring has not the precise above mentioned dimensions (in section 3), they machined by CNC milling machine to have accurate dimensions in the implemented structure exactly equal to that dimensions presented by the simulation. The groove on the surface of the ring is cut by machinery mechanic too. The next problem when implementing such kind of structures was fixing them to have a correct gap between the ring and the waveguide. Connecting the waveguide ends to the ports needs fixing too. Having centimetre dimensions this problems have been solved by themselves. The PMMA ring resonator is placed close to the PMMA waveguide by manual adjustment. Centimetre geometries both in the ports and in the tapered ends as a coupler, we connect them to each other by manual adjustment too. Figure 5 shows the final device after fabricating it.



Figure 5: The fabricated PMMA waveguide and PMMA ring resonator.

5 EXPERIMENTAL SETUP

The source wave at 8-8.3 GHz is provided by 85107A network analyzer. It has plotted the transmission parameter which is shown in figure 6 in order to calculating the ring resonator parameters, FSR and Q. It should be mentioned that the FSR can be attributed to the refractive index and loss of the PMMA. The matching between simulation and experimental transmission parameter is achieved.

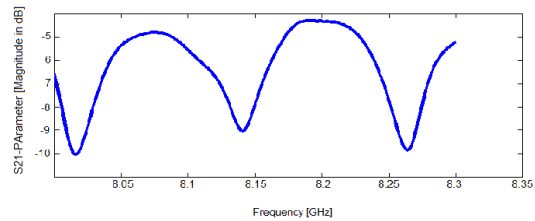


Figure 6: The plotted transmission Parameter of the ring resonator structure in the implementation.

It shows that the FSR of the ring resonator in the experiment is about 0.12 GHz and the Q-factors are about 200 and they are a bit different for each resonance peak.

The resonance frequencies are approximately the same as for the simulation. As it is visible from the comparison between simulation and fabrication there is a drop in the resonator response between resonances of the implemented structure. This is because of the attenuation that occurred by the two tapered ends, and it is unavoidable. The tapered ends are essential to have a good impedance matching between the waveguide and the ports. This impedance matching is frequency dependence of course, but the dependency could be ignored in a small frequency band such as 8-8.3 GHz. If this frequency band became larger, the variant impedance matching respect to the frequency would be visible. The other reason for the attenuation in the fabricated structure is the trivial PMMA electrical conductivity that has been assumed zero in simulation and here creates an offset in the waveguide's transmission.

The other difference which is visible in the experimental results in comparison with the simulation is lower quality factor and is due to the attenuation caused by the PMMA electrical conductivity in the ring resonator. Since we expect that Q decrease by the attenuation enhancement in the ring resonator, it is more likely that the groove geometry affects that resonator transmission function. This could be seen more obviously in figure 7. By punctuality it is seen that electromagnetic wave has some breaks in the border of PMMA and groove, but they are tolerable for the wave and the propagation don't perturbed by them. These breaks are the other reason which is beneficial for explaining the decreasing of the quality factor. The electromagnetic waves tolerate the RI differences between the groove (free space RI) and PMMA. The photon recirculation limits by this groove and this means a slaked quality factor. In implemented structure these breaks are accompanied by the electrical conductivity of the PMMA which is assumed to be zero in simulation.

Because of that the quality factors are more slaked in the fabrication.

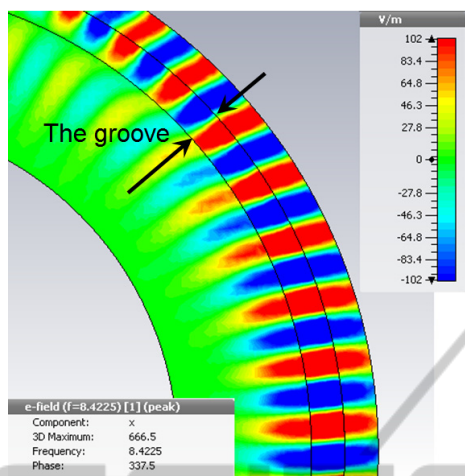


Figure 7: simulated 3D electric field (x component) distribution of the ring resonator with a groove on the surface. The electromagnetic waves break when they meet the groove.

As it can be seen from the comparison, the FSR in the experiment is lower than the simulation. This rises from a trivial difference that we have in the PMMA refractive index. Also the RI of the air in the reality is more than 1 (the assumed RI for the air in simulation). This causes that the effective RI that resonant mode in the ring experience become larger. Since FSR have an inverse relationship with the effective RI, it is predictable that FSR become lower in the experiment.

6 CONCLUSIONS

In this paper, the experimental setup and simulation results of a PMMA ring resonator and a PMMA waveguide was presented. The set of polymer based ring resonator and waveguide were designed and optimized to excite the WGM modes of the ring resonator. The centimetre range dimensions facilitate the accurate fabrication process of WGM resonator by CNC milling machine and not further manual assembly is required, which is suitable for mass production. The differences of the simulation and fabrication that are an offset in the transmission parameter and a decreasing in the quality factor rises from the attenuation that caused by the PMMA and the air electrical conductivity. The lower FSR in the experiment is the other difference that can be seen. It is because of the larger refractive indices that PMMA and air have and cause a bigger effective RI for resonance light.

REFERENCES

- Zhu, Hongying, Ian M. White, Jonathan D. Suter, Mohammad Zourob, and Xudong Fan., 2007. *Analytical chemistry* 79, no. 3, 930-937.
- Delag, Andre, Dan-Xia Xu, Ross W. McKinnon, Edith Post, Philip Waldron, Jean Lapointe, Craig Storey et al., 2009. *Journal of light wave Technology* 27, no. 9: 1172-1180.
- Ahmadi, H., H. Heidarzadeh, A. Taghipour, A. Rostami, H. Baghban, M. Dolatyari, and G. Rostami., 2014. *Optik-International Journal for light and electron Optics*.
- Yu, Zongfu, and Shanhui Fan. 2011. *Optics express* 19, no. 11:10029-10040.
- Taya, Sofyan, and Taher El-Agez. 2011, *Turk. J. Phys* 35: 31-36.
- Marcatili, Enrique AJ, 1969, *Bell System Technical Journal* 48, no. 7: 2071-2102.
- Sun, Yuze, and Xudong Fan., 2011, *Analytical and bioanalytical chemistry* 399, no 1: 205-211.
- Rabus, Dominik G., 2007. *Integrated ring resonators*, Springer.